

See discussions, stats, and author profiles for this publication at: <https://www.researchgate.net/publication/220204194>

Applying Neural Network Architecture for Inverse Kinematics Problem in Robotics

Article in *Journal of Software Engineering and Applications* · January 2010

DOI: 10.4236/jsea.2010.33028 · Source: DBLP

CITATIONS

53

READS

1,128

3 authors, including:



Bassam Daya

Lebanese University

94 PUBLICATIONS 531 CITATIONS

[SEE PROFILE](#)



Shadi Khawandi

University of Angers

24 PUBLICATIONS 138 CITATIONS

[SEE PROFILE](#)

Some of the authors of this publication are also working on these related projects:



Cyber Security via Data Mining [View project](#)



Iris Biometrics [View project](#)

Applying Neural Network Architecture for Inverse Kinematics Problem in Robotics

Bassam Daya, Shadi Khawandi, Mohamed Akoum

Institute of Technology, Lebanese University, Saida, Lebanon.
Email: b_daya@ul.edu.lb

Received November 12th, 2009; revised December 15th, 2009; accepted December 22nd, 2009.

ABSTRACT

One of the most important problems in robot kinematics and control is, finding the solution of Inverse Kinematics. Inverse kinematics computation has been one of the main problems in robotics research. As the Complexity of robot increases, obtaining the inverse kinematics is difficult and computationally expensive. Traditional methods such as geometric, iterative and algebraic are inadequate if the joint structure of the manipulator is more complex. As alternative approaches, neural networks and optimal search methods have been widely used for inverse kinematics modeling and control in robotics. This paper proposes neural network architecture that consists of 6 sub-neural networks to solve the inverse kinematics problem for robotics manipulators with 2 or higher degrees of freedom. The neural networks utilized are multi-layered perceptron (MLP) with a back-propagation training algorithm. This approach will reduce the complexity of the algorithm and calculation (matrix inversion) faced when using the Inverse Geometric Models implementation (IGM) in robotics. The obtained results are presented and analyzed in order to prove the efficiency of the proposed approach.

Keywords: Inverse Geometric Model, Neural Network, Multi-Layered Perceptron, Robotic System, Arm

1. Introduction

The task of calculating all of the joint angles that would result in a specific position/orientation of an end-effector of a robot arm is called the inverse kinematics problem. In the recent years, the robot control problem has received considerable attention due to its complexity. Inverse kinematics modeling has been one of the main problems in robotics research, there has been a lot of research on the use of neural networks for control. The most popular method for controlling robotic arms [1-5].

In inverse kinematics learning, the complexity is in the geometric and non linear equations (trigonometric equations) and in the matrix inversion, this in addition to some other difficulties faced in inverse kinematics like having multiple solutions. The traditional mathematical solutions for inverse kinematics problem, such as geometric, iterative and algebraic, may not lead always to physical solutions. When the number of manipulator degrees of freedom increases, and structural flexibility is included, analytical modeling becomes almost impossible. A modular neural network architecture was proposed by Jacobs *et al.*

and has been used by many researches [2,3,5,6].

However, the input-output relation of their networks is continuous and the learning method of them is not sufficient for the non-linearity of the kinematics system of the robot arm.

This paper proposes neural network architecture for inverse kinematics learning. The proposed approach consists of 6 sub-neural networks. The neural networks utilized are multi-layered perceptron (MLP) with a back-propagation training algorithm. They are trained with end-effector position and joint angles.

In the sections that follow, we explain the inverse kinematics problem, and then we propose our neural network approach; we present and analyze the results in order to prove that neural networks provide a simple and effective way to both model the manipulator inverse kinematics and circumvent the problems associated with algorithmic solution methods.

The proposed approach is presented as a strategy that could be reused and implemented to solve the inverse kinematics problems faced in robotics with highest degrees of freedom. The basics of this strategy are explained in details in the sections that follow.

2. Inverse Kinematics Problem

Inverse kinematics computation has been one of the main problems in robotics research. This problem is generally more complex for robotics manipulators that are redundant or with high degrees of freedom. Robot kinematics is the study of the motion (kinematics) of robots. They are mainly of the following two types: *forward kinematics* and *inverse kinematics*. Forward kinematics is also known as direct kinematics. In forward kinematics, the length of each link and the angle of each joint are given and we have to calculate the position of any point in the work volume of the robot. In inverse kinematics, the length of each link and position of the point in work volume is given and we have to calculate the angle of each joint. In this section, we present the inverse kinematics problem.

2.1 Inverse Position Kinematics and IGM

The inverse position kinematics (IPK) solves the following problem: "Given the desired position of the robot's hand; what must be the angles at the robot joints?" In contrast to the forward problem, the solution of the inverse problem is not always unique: The same end effector's pose can be reached in several configurations, corresponding to distinct joint position vectors. The conversion of the position and orientation of a robot manipulator end-effector from Cartesian space to joint space is called inverse kinematics problem. For any position in the X-Y plane for a 2R robot, there is a possibility of 2 solutions for any given point. This is due to the fact that there are 2 configurations that might be possible to reach the desired point as **Figure 1**.

The math involved in solving the Inverse Kinematics problem requires some background in linear algebra, specifically in the anatomy and application of transformation matrices.

Therefore, an immediate attempt to solve the inverse kinematics problem would be by inverting forward kinematics equations.

Let's illustrate how to solve the inverse kinematics problem for robot manipulators on a simple example. **Figure 2** shows a simple planar robot with two arms. The underlying degrees of freedom of this robot are the two angles dictating the rotation of the arms. These are labeled in **Figure 2** as θ_1 and θ_2 . The inverse kinematics question in this case would be: What are the values for the degrees of freedom so that the end effector of this robot (the tip of the last arm) lies at position (x, y) in the two-dimensional Cartesian space? One straightforward approach to solving the problem is to try to write down the forward kinematics equations that relate (x, y) to the two rotational degrees of freedom, then try to solve these equations. This solution, named **IGM** (Inverse Geometric Model) will give us an answer to the inverse kinematics problem for this robot. The calculation is presented in **Figure 3**.

As it can be seen in the example above, the solutions to

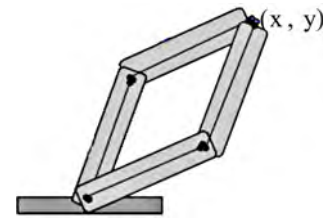


Figure 1. Two solutions depicted for the inverse kinematics problem

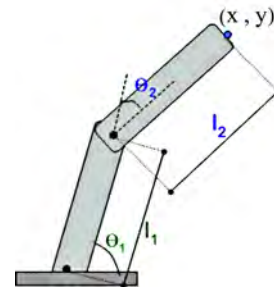


Figure 2. Steer end-effector (x, y) target position

$$x = l_1 \cos(\theta_1) + l_2 \cos(\theta_1 + \theta_2)$$

$$y = l_1 \sin(\theta_1) + l_2 \sin(\theta_1 + \theta_2)$$

$$x^2 + y^2 = l_1^2 + l_2^2 + 2l_1 l_2 \cos(\theta_2)$$

$$\cos(\theta_2) = \frac{x^2 + y^2 - l_1^2 - l_2^2}{2l_1 l_2}$$

$$x = l_1 \cos(\theta_1) + l_2 (\cos(\theta_1) \cos(\theta_2) - \sin(\theta_1) \sin(\theta_2))$$

$$x = \cos(\theta_1) (l_1 + l_2 \cos(\theta_2)) - \sin(\theta_1) (l_2 \sin(\theta_2))$$

$$y = \cos(\theta_1) (l_2 \sin(\theta_2)) + \sin(\theta_1) (l_1 + l_2 \cos(\theta_2))$$

$$\cos(\theta_1) = \frac{x + \sin(\theta_1) l_2 \sin(\theta_2)}{l_1 + l_2 \cos(\theta_2)}$$

$$\sin(\theta_1) = \frac{(l_1 + l_2 \cos(\theta_2))y - l_2 \sin(\theta_2)x}{l_1^2 + l_2^2 + 2l_1 l_2 \cos(\theta_2)}$$

Figure 3. Finding solutions from the forward kinematics equations

an inverse kinematics problem are not necessarily unique. In fact, as the number of degrees of freedom increases, so does the maximum number of solutions, as depicted in the figure. It is also possible for a problem to have no solution if the point on the robot cannot be brought to the target point in space at all.

While the above example offers equations that are easy to solve, general inverse kinematics problems require solving systems of nonlinear equations for which there are no general algorithms. Some inverse kinematics problems

cannot be solved analytically. In robotics, it is sometimes possible to design systems to have solvable inverse kinematics, but in the general case, we must rely on approximation methods in order to keep the problem tractable, or, in some cases, even solvable.

It is known that there is a finite number of solutions to the inverse kinematics problem. There are, however, 3 types of solutions: complete analytical solution, numerical solutions and semi-analytical solution. In the first type, all of the joint variables are solved analytically according to given configuration data. In the second solution type, all of the joint variables are obtained iterative computational procedures. There are four disadvantages in these: 1) incorrect initial estimations, 2) before executing the inverse kinematics algorithms, convergence to the correct solution cannot be guaranteed, 3) multiple solutions are not known, 4) there is no solution, if the Jacobian matrix is singular. In the third type, some of the joint variables are determined analytically and some computed numerically. Disadvantage of numeric approaches to inverse kinematics problem is also heavy computational calculation and big computational time.

3. Neural Network Approach

The true power and advantage of neural networks lies in their ability to represent both linear and non-linear relationships and in their ability to learn these relationships directly from the data being modeled. Traditional linear models are simply inadequate when it comes to modeling data that contains non-linear characteristics. The most common neural network model is the multilayer perceptron (MLP). This type of neural network is known as a supervised network because it requires a desired output in order to learn. The goal of this type of network is to create a model that correctly maps the input to the output using historical data so that the model can then be used to produce the output when the desired output is unknown. A graphical representation of an MLP is shown in **Figure 4**.

The MLP and many other neural networks learn using an algorithm called back propagation. With back propagation, the input data is repeatedly presented to the neural network. With each presentation the output of the

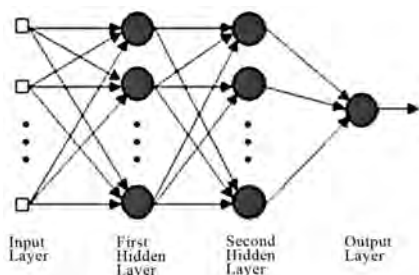


Figure 4. A two hidden layer multilayer perceptron (MLP)

neural network is compared to the desired output and an error is computed. This error is then fed back (back propagated) to the neural network and used to adjust the weights such that the error decreases with each iteration and the neural model gets closer and closer to producing the desired output. This process is known as “training”.

As mentioned previously, for any position in the X-Y plane for a 2R robot, there is a possibility of 2 solutions, so our approach started by implementing one sub-networks for each solution. For each network, we will try to obtain from the DGM model a series of q_1 (or θ_1) and q_2 (or θ_2) for a given position of the end-effector. The data training for the 2 sub-networks will be constructed as following:

- Neural Network NN1: $(x, y) \rightarrow (q_1, q_2)$;
 - q_1 between 0 and 2π , and q_2 between 0 and π .
- Neural Network NN2: $(x, y) \rightarrow (q_1, q_2)$;
 - q_1 between 0 and 2π , but q_2 between $-\pi$ and 0.

As we are going to use DGM for generating our input parameters for the MLP (q_1 and q_2), for singular configurations, for the same point X and Y, there are two solutions for it within the same aspect. For example, as shown in **Figure 5**, for 2 close positions of (x, y) we have big difference in q_1 values (first value of q_1 is close to 0 and the other q_1 is close to 2π). Thus, this will create a problem during training for our data.

So the above implementation (2 neural networks) leads to a big difficulty in the learning process. In order to solve this problem, we will use 4 Neural Networks (MLP); one for each quadrant.

By implementing 4 Neural Networks (MLP), we prevent two main problems: 1) no more problem to construct the training data for each aspect, and 2) no more problem in the learning phase (one output for one input).

For the error there will be two other Neural Networks:

- One for the Cartesian space (MLP5), used to classify whether the given position is within or not in the accessible region. The error will be representing whether the given solution is within the limitation of the robots.
- One for the joint space (MLP6) to respect the joint limits of our robot.

The approach will use the schematic of the neural network architecture given in **Figure 6**. The DGM model is used to handle the problem of identifying which MLP from the four MLPs is giving the right answer.

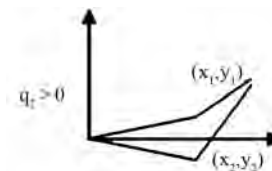


Figure 5. Two close positions for (x, y) but too different values for q_1 (0 and 2π) and this is for the same Neural Network NN1 ($q_2 > 0$)

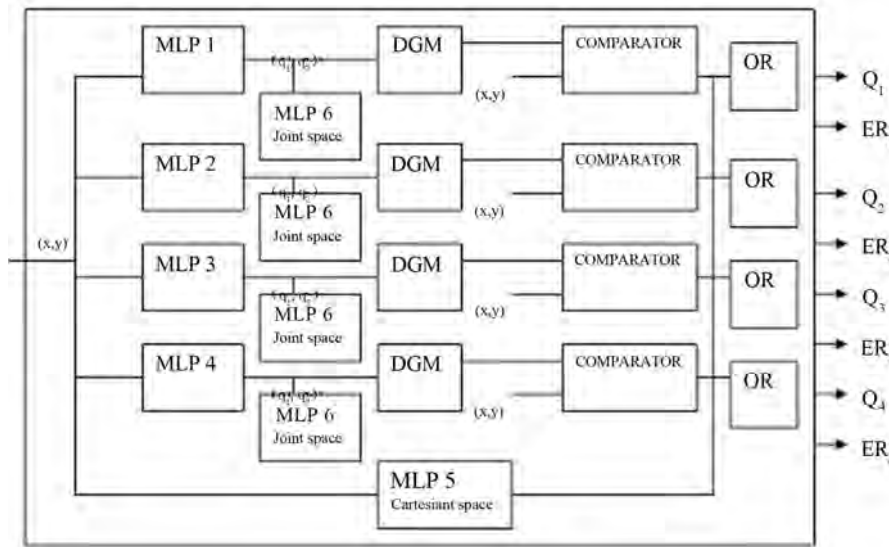


Figure 6. Multi-layer perceptron architecture using 4 MLPs (1 to 4) for the 4 quadrants, MLP5 for the Cartesian space and MLP6 for the joint space. Q_i represent the output (q_1, q_2) for MLP $_i$ ($i = 1$ to 4) and ER_i represent the error output (if $ER_i = 0$ then Q_i accepted; if $ER_i = 1$ then Q_i rejected).

4. Training, Experiments and Results

In this section, we present the configuration and preparing of the neural network, and the experiments, with their results, executed in this approach.

We will use 6 MLPs to solve this problem. There will be 1 MLP for each quadrant of the joint space, as shown in Figure 7, mainly for q_1 positive and q_2 positive, q_1 negative and q_2 positive, q_1 positive and q_2 negative and lastly q_1 negative and q_2 negative. For the error there will be 2 other neural networks: one to classify whether the given position is within accessible region and one for the joint space.

4.1 Creating MLP Network for IGM of 2R Planar Robot

As mentioned above, for any position in the X-Y plane for a 2R robot, there is a possibility of 2 solutions for any given point. The approach will try to obtain a series of q_1 and q_2 for a given position of the end-effector in the X-Y plane. This is due to the fact that there are 2 configurations that might be possible to reach the desired point.

For this MLP problem, we will be using 12 neurons for the first layer and 8 neurons for the second layer and 2 neurons for the output. However, the difference is that we will be using 6 MLPs to solve this problem. There will be 1 MLP for each quadrant of the joint space, as shown in Figure 7, mainly for ($q_1 > 0$ and $q_2 > 0$), ($q_1 > 0$ and $q_2 < 0$), ($q_1 < 0$ and $q_2 > 0$) and lastly ($q_1 < 0$ and $q_2 < 0$).

This is done due to the fact that we are going to use DGM for generating our input parameters for the MLP(q_1 and q_2). For singular configurations, for the same point

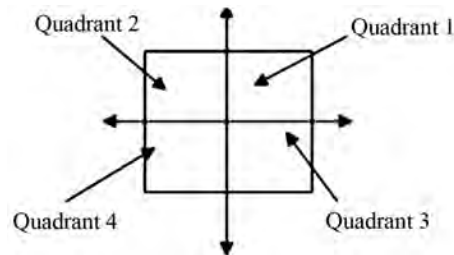


Figure 7. X-Y plane in 4 quadrants

X and Y, there are two solutions for it within the same aspect. For example, for $q_1 = \pi$ and $q_2 = -\pi$, they will have the same X and Y for any value of q_2 . Thus, this will create a problem during training for our data. Thus, to solve this problem, we will be using one MLP for each quadrant of data. For the error there is perceptron used to classify whether the given X and Y is within accessible and non accessible region. The error will be representing whether the solution given is within the limitation of the robots. For example, if we give a point inside the non-accessible region of the working space, the error will be 1 and -1 for inside the accessible region.

For each quadrant, we created 10 variables for our target between $q_1 = 0$ to π and equivalently for q_2 . Then, we will use the Direct Geometry Model (DGM) function to generate the data training for our MLPs. The tansig function, used in our MLPs, will have its input from +3 to -3 and its output between +1 and -1. The input and output for the MLP is then scaled according to the tansig function.

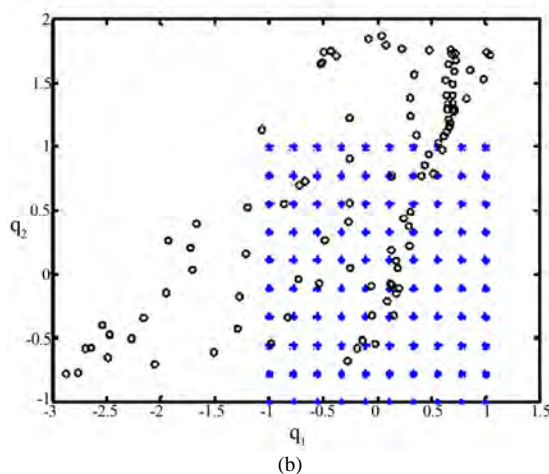
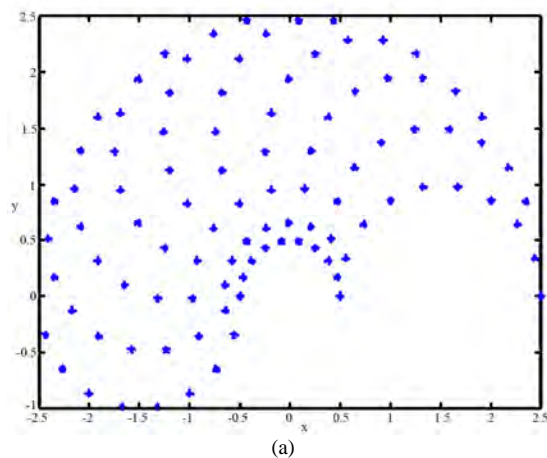
To achieve this, we multiply the input x by 2.5 such that, we will obtain $-3 < x \cdot 2.5 < 3$ (the same for the 4 MLPs). The other scaling is given in Table 1.

Table 1. Scaling of the input y and the outputs q_1 and q_2 for each MLP according to the tansig function

No. MLP	q_1	q_2	Y
MLP1	$-1 < (q_1 \cdot 2\pi) - 1 < 1$	$-1 < (q_2 \cdot 2\pi) - 1 < 1$	$-3 < (y \cdot 5) - 2 < 3$
MLP2	$-1 < (q_1 \cdot 2\pi) + 1 < 1$	$-1 < (q_2 \cdot 2\pi) - 1 < 1$	$-3 < (y \cdot 5) + 2 < 3$
MLP3	$-1 < (q_1 \cdot 2\pi) - 1 < 1$	$-1 < (q_2 \cdot 2\pi) + 1 < 1$	$-3 < (y \cdot 5) - 2 < 3$
MLP4	$-1 < (q_1 \cdot 2\pi) + 1 < 1$	$-1 < (q_2 \cdot 2\pi) - 1 < 1$	$-3 < (y \cdot 5) + 2 < 3$

4.1.1 The First MLP for the First Quadrant

For the first quadrant, we created 10 variables for our target between $q_1 = 0$ to π and equivalently for q_2 . Then, we will use our DGM2R function to generate the input for our MLP. The input and output for the MLP is then scaled according to the tansig function. The tansig function will have its input from +3 to -3 and its output between +1 and -1. To achieve this, will be dividing our output and multiplying our inputs with factors. The resulting input and output of for the MLP is shown in **Figure 8**.

**Figure 8. (a) Input for first quadrant MLP; (b) target output for first quadrant MLP**

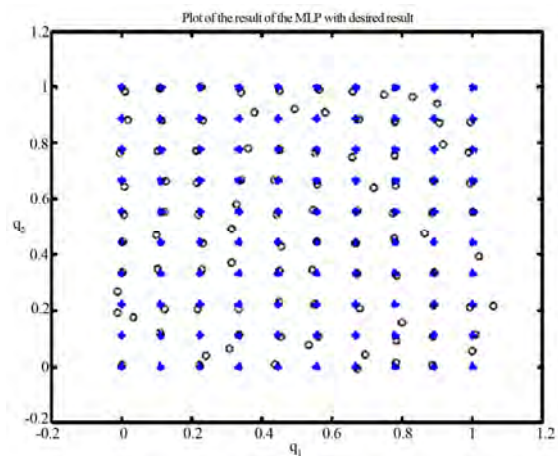
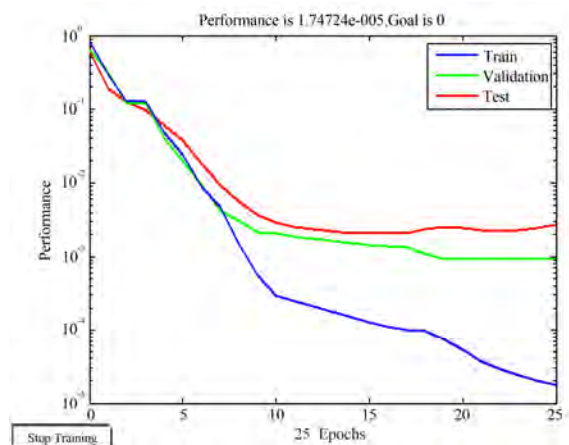
It is shown as well in **Figure 8** that the initial result from our MLP prior to training. For our MLP, we will be using “trainlm” function since it is faster and more accurate in producing the result.

The MLP managed to produce accurate data with error of 1.74×10^{-5} within 25 epochs. The result is then plotted back to our target. **Figure 9** shows the result for the MLP restoring the data prior to scaling. From **Figure 9**, we know that our MLP has managed to produce quite an accurate result since the result of the MLP is pretty close to our target values.

For this MLP, we have used learning rate equal to 0.2. The performance of the MLP is shown in **Figure 10**.

4.1.2 The Second MLP for the Second Quadrant

In the second MLP for the second quadrant of the joint limit, we will do the same algorithm for training the MLP. We will input our data in the range of q_1 from 0 to -2.8 and q_2 from 0 to π . We will then input our data to “tansig” transfer function. The inputs and outputs as well the initial output of our MLP are presented in **Figure 11**. Using the

**Figure 9. Result of the first quadrant MLP plotted onto the target data****Figure 10. Performance result for this first MLP**

“trainlm” function, we managed to obtain accuracy of 1.38×10^{-5} within 41 epochs.

The result of the MLP is presented in **Figure 12**. The result of the MLP presented is prior to rescaling back to the original data. For the third MLP we will be performing the similar operation by scaling the input and the output before inputting it to the MLP to be learnt.

4.1.3 The Third MLP for the Third Quadrant

For the third MLP, we are trying to generate result for q_1 in the range of 0 and π and q_2 in the range of 0 to -2.8 . We are using -2.8 because of the requirement of the joint limit present in the system. The initial input and output of the system is presented in the following **Figure 13**.

After training our MLP for 15 epochs, we managed to get an error in performance of 4.64×10^{-5} . The plot of the result and the plot of the outputs are given in the following **Figure 14**.

4.1.4 The Fourth MLP for the Fourth Quadrant

For the last MLP to generate the result for IGM model, we

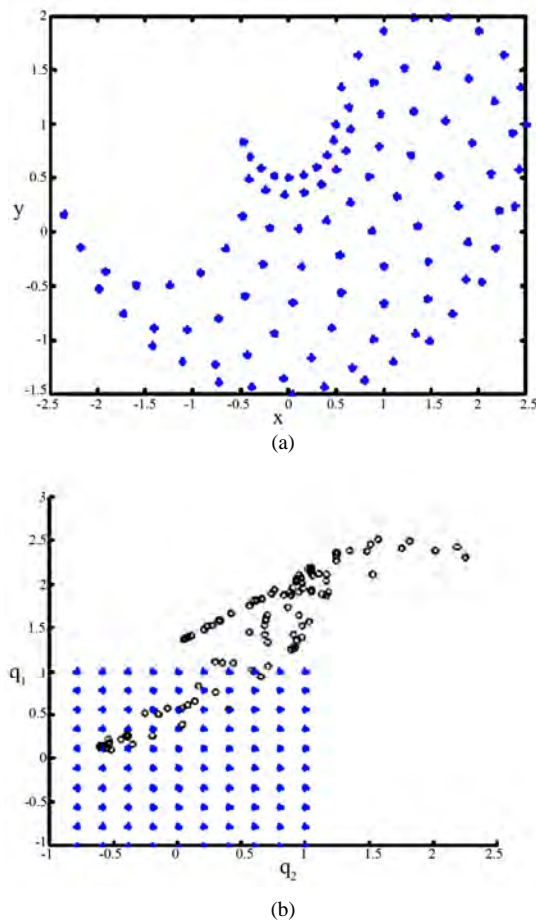


Figure 11. (a) Input data for the second quadrant MLP; (b) output of the second MLP plotted together with the desired result

are trying to generate result for q_1 in the range of 0 and -2.8 and q_2 in the range of 0 to -2.8 . For the same reason, we are using -2.8 because of the requirement of the joint limit present in the system. The initial input and output of the system is presented in **Figure 15**. After training for 13 epochs, we managed to get an error of 5.24×10^{-5} and the result of the MLP is plotted against the desired result. We can observe that the resulting points from the MLP are close to the desired target. The result of the MLP and the performance of the MLP are presented in **Figure 16**.

4.1.5 The Fifth MLP

The fifth MLP is designed to define the workspace of the robot. The robot workspace is a circle with an internal circle upon which the robot will not be able reach. Thus, there is a limitation to the area upon which the robot is able to access the area. When the given x and y is within the internal circle or outside the working circle as depicted in **Figure 17**, the error of the equation will be 1.

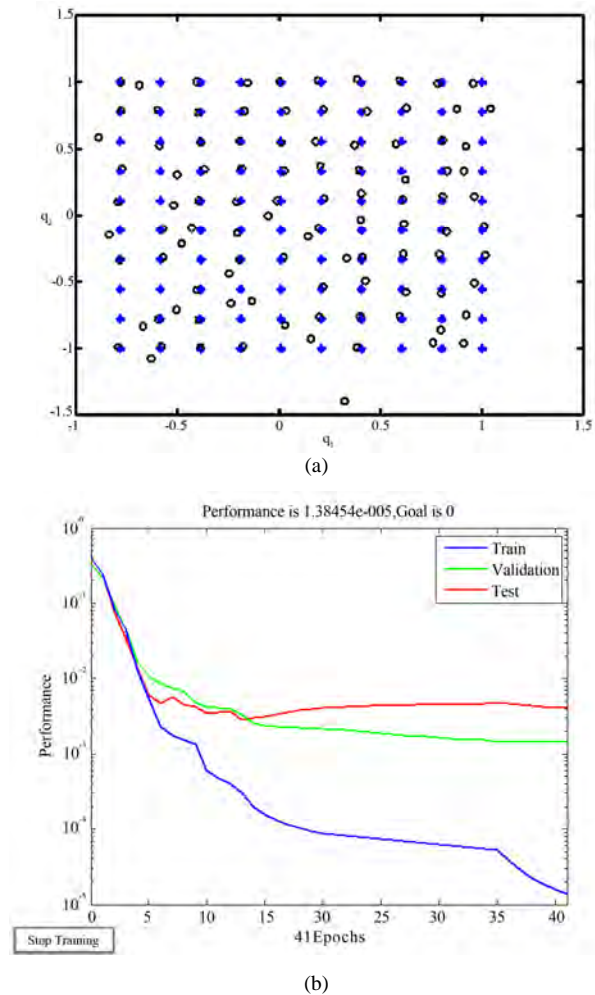


Figure 12. (a) Result of MLP plotted with the desired target; (b) Performance of MLP with trainlm function

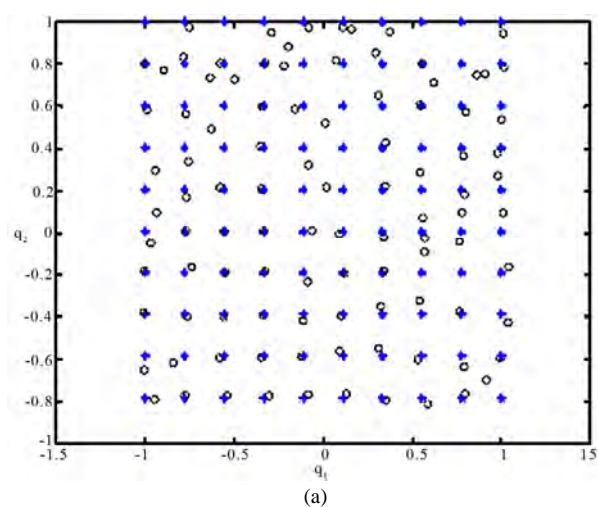
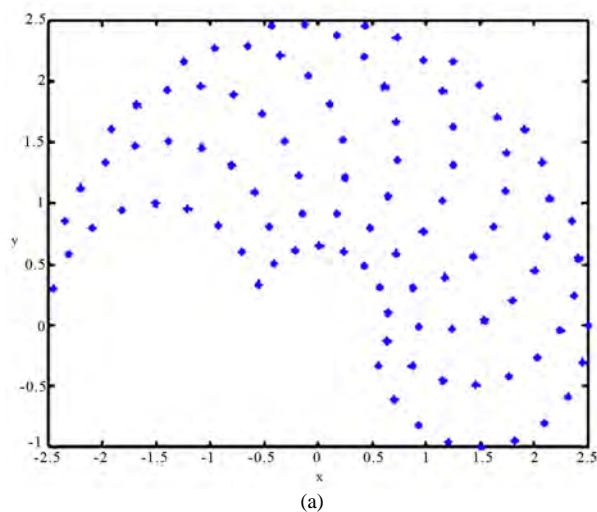


Figure 13. (a) Input for the 3rd MLP; (b) output of the 3rd MLP plotted with the desired result

In order to do this, we will find the relationship between the length of the robots arms to the radius of its working space. We know that the radius of the large circle is given by the formula $R=L_1+L_2$. Thus, we know that within the gray circle, $(R-L_1)^2=L_2^2$. Expanding the equation, we know that $R^2-2L_1L_2+(L_1^2+L_2^2)=0$.

Thus, we notice that if the desired point is within the gray area, the value of the equation above will be less than 0, and otherwise if the value of R is smaller than L_1-L_2 or R is greater than L_1+L_2 .

We have created 20 numbers of data of X_1 and X_2 for the input to the MLP.

Then, using these inputs, we calculate our desired target using the “error3” function using a notation that if *error* is 1 then the point is not inside working circle and if *error* is 0 then the robot is inside the working circle. The desired target is presented in **Figure 18**. Our result shows that

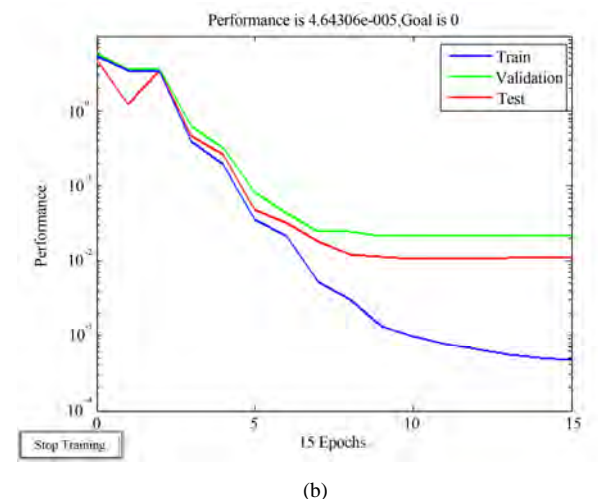


Figure 14. (a) Output of the result plotted together with the desired target of the 3rd MLP; (b) Performance of the 3rd MLP

the MLP has managed to classify the classes within 17 epochs with zero error. Thus, this error problem has been solved with only a single perceptron. The result of the MLP is presented in **Figure 18**.

The performance of the perceptron is shown in **Figure 19**.

4.1.6 The Sixth MLP

The last step of the classification is to categorize the resulting Q_1 and Q_2 into either $[0\ 0]$, $[0\ 1]$ or $[1\ 0]$. This means on the other hand, we need to classify the elements of angles in the Q_1 and Q_2 . If we draw the boundary limit of the angles, we would be able to find a rectangular area (as shown in **Figure 20**). Certainly, we can apply the method of perceptron with 3 layers for implementing classifier arbitrary linearly limited areas (polyhedron).

Thus, if our MLP is having 4 neurons on the first layer and 1 neuron on the second layer and taking Q_1 and Q_2 as the input parameters for the neuron and output of 1 if Q_1 or

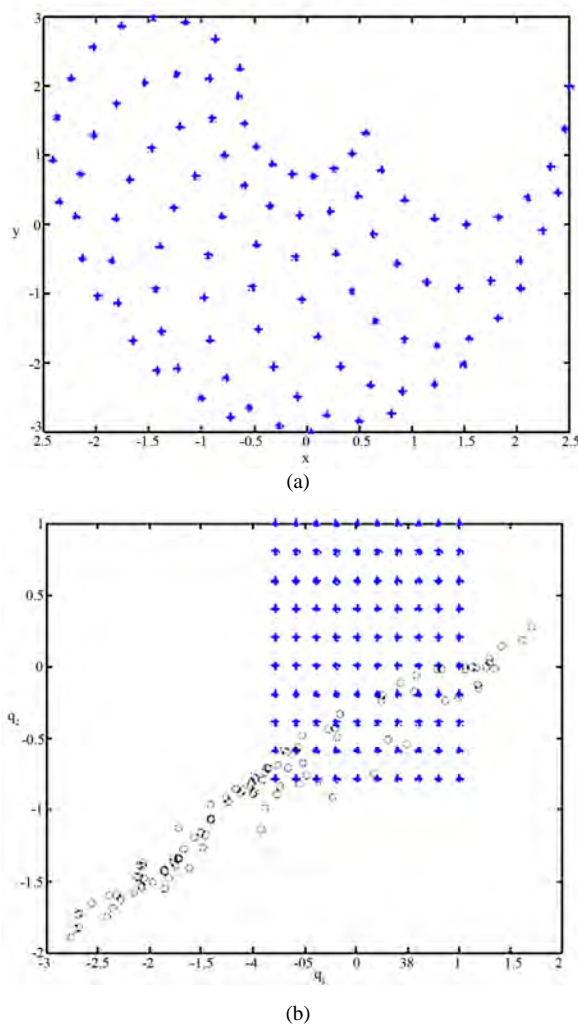


Figure 15. (a) Input to the 4th MLP; (b) initial output of the 4th MLP plotted together with the desired result

Q_2 is within the grey area and -1 if it outside the gray area, we should be able to fully classify the problem.

The weights of our neurons are given as follows:

$$W^1 = \begin{bmatrix} 1 & 0 \\ 1 & 0 \\ 0 & 1 \\ 0 & 1 \end{bmatrix}, \text{ and } b^1 = \begin{bmatrix} -3 \\ 2.8 \\ -3 \\ 2.8 \end{bmatrix}$$

Marking the desired area (grey area), we obtained

	g_1	g_2	g_3	g_4
G_1	-	+	-	+

Thus, $W^2 = [-1 \ 1 \ -1 \ 1]$, and $b^2 = [-3]$.

From this weights and biases, our convention is :

- output = 1 if the value of Q is within the joint limit.
- output = -1 if the value of Q is outside the joint limit.

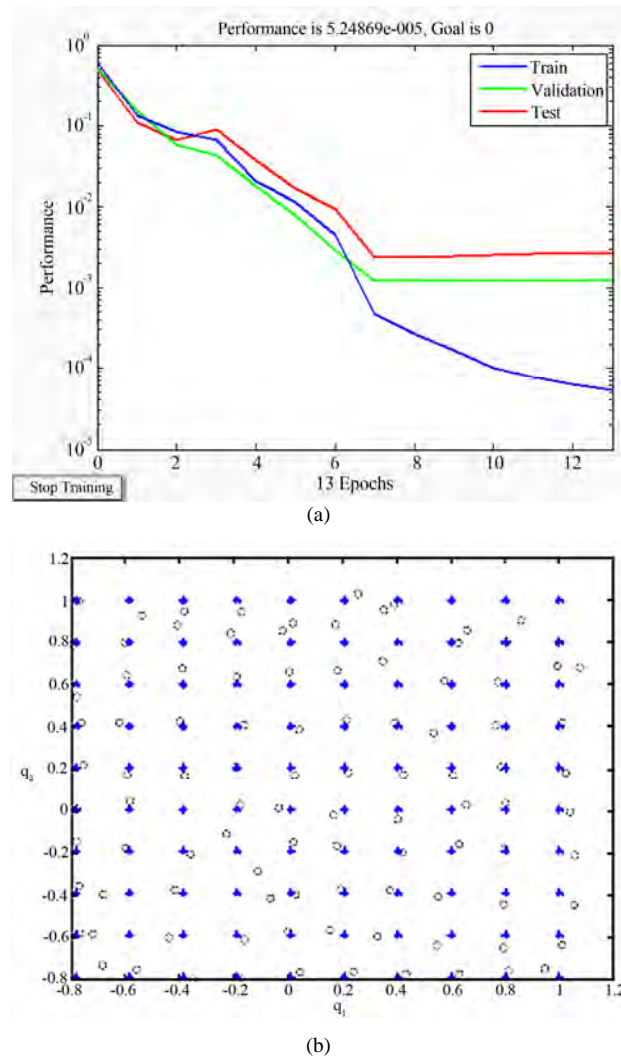


Figure 16. (a) Performance of the 4th MLP; (b) Result of the 4th MLP plotted together with the desired target

With these values, we can create a MLP network and we will be able to separate the two results perfectly. The result is shown in **Figure 21**. Lastly, the final step is to combine all the 6 MLP together in a program that we can use to generate the desired Q_1 and Q_2 and error. We will need to classify for the y of the input to our joint network. Initially, when the input is having $y > 0$, there are two solutions that are possible, which is q_1 is positive and q_2 is positive or negative. Thus, we have to choose quadrant 1 or 4 to obtain a correct result. Otherwise, when $y < 0$, the two solutions that are possible are q_1 is negative and q_2 is positive or negative. After we have done the classification, then we can use our network to produce the desired result. The program will check whether the given X and Y is within the working circle. If it does not, then the error will be equal to $[1 \ 1]$ and the value of Q_1 and Q_2 will be of a null vector. On the other hand, if the point X, Y is within

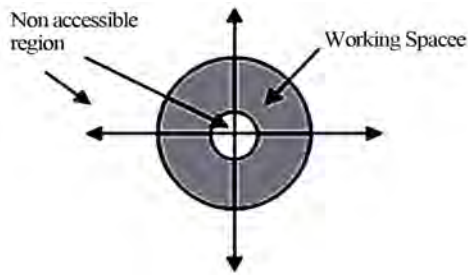


Figure 17. Working space of the robot

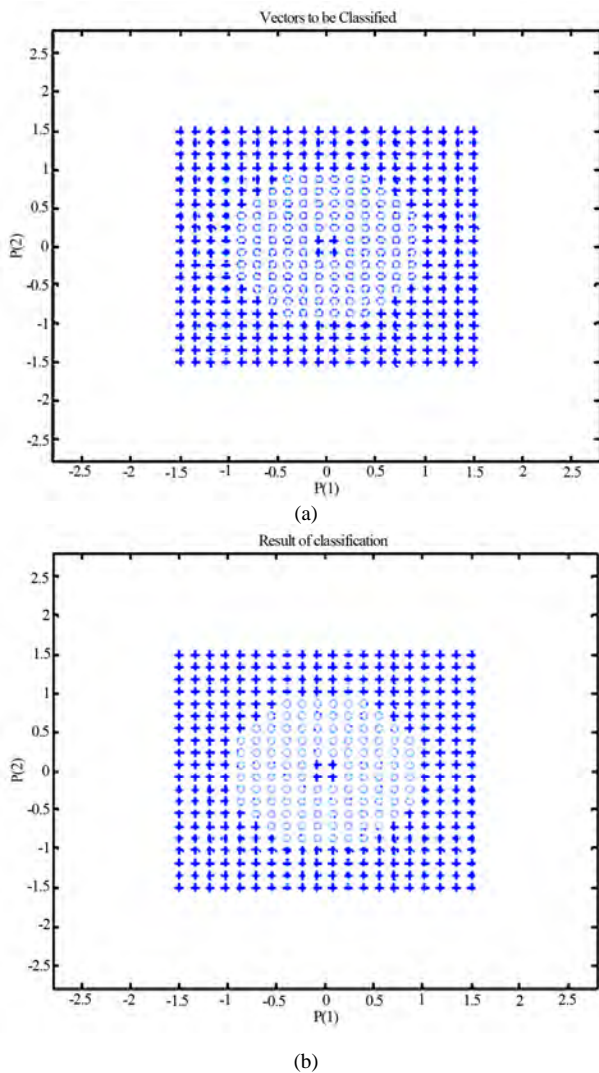


Figure 18. (a) Desired target result; (b) Result of the MLP

the circle, then it will input the X and Y according to the given area as described above. Then, the resulting result will be fed into the MLP 6 for determining whether the result is within the joint limit or not. If it does, then error will be equal to 0 and if it is not in the joint limit, then error will be equal to 1.

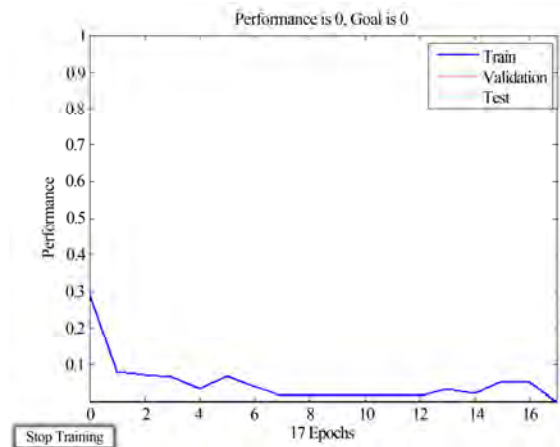
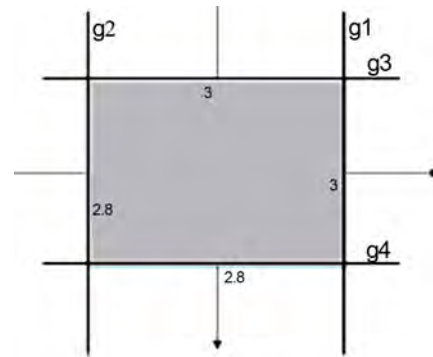


Figure 19. Performance of the perceptron

Figure 20. Classification to categorize Q_1 and Q_2

Testing the MLP with values of $X = [0.646 \ -0.3196]$ which corresponds to $q = [-\frac{\pi}{3} \ \frac{\pi}{2}]$, we obtained from our MLP,

$$Q_1 = [1.0936 \ 1.6016]$$

and

$$Q_2 = [2.2538 \ -1.5618]$$

Our optimum result for the Q_1 and Q_2 from the IGM model is

$$Q_1 = [1.047 \ 1.570]$$

and

$$Q_2 = [2.2232 \ -1.5708]$$

We know that the value from of MLP is pretty close to the real values of the IGM2R model. The error is $[0 \ 0]$ and $[0 \ 0]$ respectively.

Testing the MLP with values of

$$X = [-0.3196 \ -0.6464]$$

which corresponds to $q = [-\frac{5\pi}{6} \ \frac{\pi}{2}]$, we obtained from our MLP,

$$Q_1 = [-2.6856 \quad 1.8241]$$

and

$$Q_2 = [-1.4809 \quad -1.6115]$$

Our optimum result for the Q_1 and Q_2 from the IGM model is

$$Q_1 = [-2.6180 \quad 1.5708]$$

and

$$Q_2 = [-1.4420 \quad -1.5708]$$

We know that the value from of MLP is pretty close to the real values of the IGM2R model. The error is [0 0] and [0 0] respectively.

5. Conclusions

In this paper, experimental results on the control of ro-

botic manipulator using neural networks have been provided and it has been demonstrated that neural networks do indeed fulfill the promise of providing model-free learning controllers for robotic systems and provide an excellent alternative for the control of robotic manipulators.

Here, neural network model (MLP) solve the issues faced when the Inverse Geometric Model (IGM) is used, which requires no matrix inversion and iterates directly on the joint position, being thus suitable for on-line application and also preserving repeatability. In other words, Multilayer Networks are applied to the robot inverse kinematics problem. The networks are trained with end-effector position and joint angles. After training, performance is measured by having the network generate joint angles for arbitrary end-effector trajectories.

It is found that neural networks provide a simple and effective way to both model the manipulator inverse kinematics and circumvent the problems associated with algorithmic solution methods.

The proposed approach in the paper can be treated as a strategy to be followed for any other future work in the same domain. Mainly it can be implemented for robotics manipulators that are redundant or with high degrees of freedom. It is useful to mention that, based on the proposed approach; new research has been started lately for applying neural networks approach for 3R robotics.

REFERENCES

- [1] B. Choi and C. Lawrence, "Inverse kinematics problem in robotics using neural networks," National Aeronautics and Space Administration, Lewis Research Center, Cleveland, 1992.
- [2] R. Köker, C. Öz, T. Çakar, and H. Ekiz, "A study of neural network based inverse kinematics solution for a three-joint robot," *Robotics and Autonomous Systems*, Vol. 49, pp. 227–234, 2004.
- [3] L. Wei, H. Wang, and Y. Li, "A new solution for inverse kinematics of manipulator based on neural network," *Machine Learning and Cybernetics*, Vol. 2, pp. 1201–1203, 2003.
- [4] J. Guo and V. Cherkassky, "A solution to the inverse kinematic problem in robotics using neural network processing," *International Joint Conference on Neural Networks*, Vol. 2, pp. 299–304, 1989.
- [5] D. Pham, M. Castellani, and A. Fahmy "Accountability learning the inverse kinematics of a robot manipulator using the Bees Algorithm," *6th IEEE International Conference on Industrial Informatics*, pp. 493–498, 2008.
- [6] E. Gallaf, "Multi-fingered robot hand optimal task force distribution: Neural inverse kinematics approach," *Robotics and Autonomous Systems*, Vol. 54, No. 1, pp. 34–51, 2006.

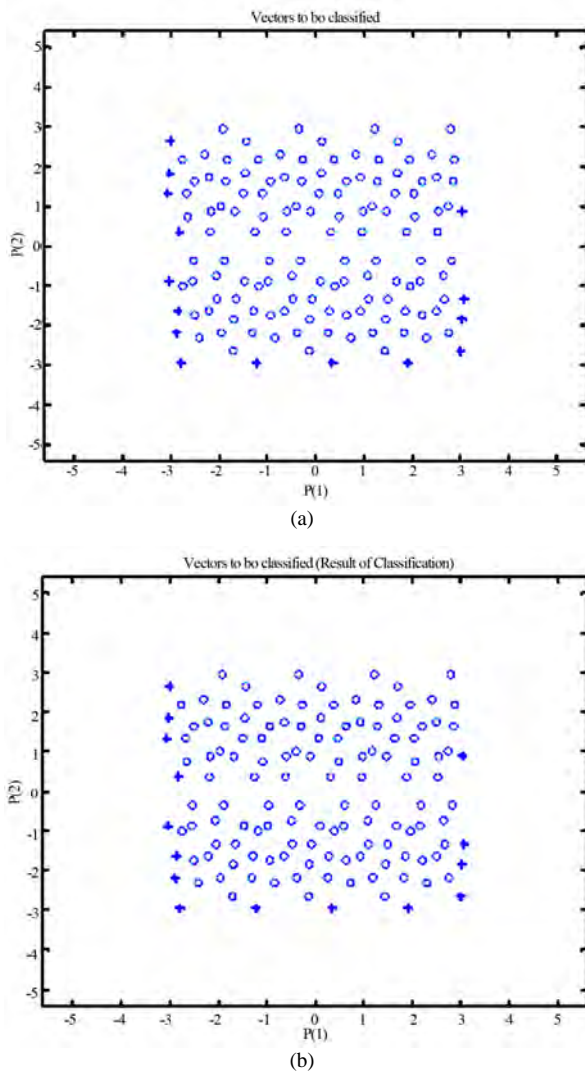


Figure 21. (a) Plot of the input Q with the desired classification; (b) Plot of the input Q with the result of classification